SMALL GRID EFFECT ON MOTOR SCHEMA-BASED MODEL FOR PEDESTRIAN FLOW WITH DIFFERENT WALK VELOCITIES

W.G. Weng[1], S. Tsuchiya[2], H.Y. Yuan[1], W.C. Fan[1] and Y. Hasemi[2]
[1] Center for Public Safety Research, Department of Engineering Physics, Tsinghua University Beijing, 100084, P.R. China
[2] Department of Architecture, Waseda University, Okubo 3-4-1, Shinjuku-ku, Tokyo, 169-8555, Japan

ABSTRACT

Motor schema-based cellular automaton model for pedestrian and evacuation dynamics states that each pedestrian is treated as an intelligent mobile robot, and motor schemas including move-to-goal, avoid-away and avoid-around drive pedestrians to interact with their environment. Small grid analysis of this model for the check of the effect of different numbers of small grid at an update time-step with the same desired walk velocity, on the travel time, is conducted. Experiments of unidirectional pedestrian flow with different walk velocities were carried out to validate the presented model. The lower walk velocity was provided by the normal people with special equipment, which made them walk slowly, to imitate the elderly people. Firstly the walk velocities of the normal people and the imitated elderly people were measured. Travel time of each pedestrian from start line to goal line was measured to compare with simulation results. The comparison results indicate that the experimental observations can be well reproduced with the motor schema-based cellular automaton model. And the simulation results of the mean travel time with one small grid at an update time-step agree well with the experimental data. It illustrates that the presented motor schema-based cellular automaton model with an appropriate small grid at an update time-step is efficient in the simulation of pedestrian flow and is a useful tool for fire safety research and management.

KEYWORDS: Motor schema, Pedestrian flow, Human behavior

INTRODUCTION

From the early 1990s until recently, with the development of economy, high-rise buildings and densely populated occupancies have become the major features of new constructions in China. However, fire hazard associated with these buildings is becoming more and more serious. On account of the large occupancy in buildings, crowd disasters, in terms of multiple death and injury, have become one of the main risks in building fire. The 9/11 incident in the USA was not the only disaster that attracted the attention of government to human evacuation in fire. The fires in the Luoyang Dongdu Commercial Building (309 deaths) and Xinjiang Kelamayi Hall (323 deaths) all attracted great attention with respect to human evacuation from almost social group, including government, fire fighters, planners, engineers and building occupants.

Recently approaches based on cellular automaton (CA) and lattice gas (LG) have been suggested to investigate pedestrian and evacuation dynamics [1-8]. These models can be divided into two types, one is based on biased-random ideas [1-5], and another is inspired from the process of chemotaxis as used by some insects[6-8]. Weng et al. have presented a behavior-based (motor schema-based) cellular automaton model for pedestrian dynamics [9]. The idea of behavior-based model is from Brooks's behaviorism for mobile robots, based on which Brooks developed subsumption architecture[10] and Arkin presented motor schemas [11]. Since CA model is discrete, the different move distance at an update time-step will result in different travel times of pedestrians though almost all CA (LG) models have the same move distance as the lattice spacing. Kirchner et al. investigated the influence of the interaction range and the spatial discretization[8]. For the former one, they simulated pedestrian movement through letting pedestrian move more than one cell; for the latter one, they combined with a reduction of the cell size to study the effect of small move distance at an update time-step. Weng et al. also did small grid analysis of a discrete model (biased-random model) for evacuation from a hall to check the effects of different desired walk velocities with the same walk time at an update time-step, and different numbers of small grid at an update time-step with the same desired walk velocity, on the evacuation time [12]. This paper conducts small grid analysis for validation of the motor schema-based CA model through experiments.

However, the above pedestrian flows are all homogeneous, i.e. the same walk velocity for all pedestrians. In practices, the pedestrian flow is heterogeneous. When the flow includes normal people and elderly people, since slower pedestrians hold back faster ones, faster pedestrians usually swirl over and exceed the slower ones. Thus it is important to study the heterogeneous pedestrian flow, especially for the interaction among pedestrians with different walk velocities. Weng, et al. ever studied the pedestrian counter flow dynamics with different walk velocities considering periodic and open boundary conditions [13]. In this paper, we study the unidirectional pedestrian flow with different walk velocities numerically and experimentally. The next section gives experimental setup (initial distribution of pedestrians including normal people and imitated elderly people) and experimental data. Section 3 describes the modes including outline of motor schema-based cellular automaton models and small grid ideas, and also presents the simulation results, followed by Conclusions in Section 4.

EXPERIMENTS

We have experimentally studied the unidirectional pedestrian flow in Waseda University, Japan, which is schematically illustrated in Fig. 1. In the whole walk way, there are the start zone, the approach zone, the start line, the walk zone, the obstacle and the goal line. In the start zone with $L_s = 3$ m and $W_s = 2$ m, pedestrians with two different walk velocities are distributed into a certain pattern. The dark full circle represents the normal people, and the black one indicates the elderly people. The approach zone, whose length is $L_a = 5$ m and configuration takes on a trapezium, is set to let pedestrian walk to a narrower walk zone from start zone. In the walk zone of length $L_w = 15$ m and width $W_w = 1.4$ m, there are two situations including no obstacle and both-side obstacle with width of 0.9 m. For the elderly people, it is impossible to let the true elders walk in the walk zone because a large number of experiments will make them tired. We used the normal people with special equipment, which made them walk slowly, to imitate the elderly people. The equipment includes goggles, earplugs, elbow-pads, and weights attached on the wrist, kneepad, ankle and crutch, shown in Fig. 2. The equipment is used not only to make normal people walk slowly, but also to describe the elderly people's other characteristics, i.e. some blind and deaf, etc. Here we concentrated on pedestrian flow between start line and goal line.

Firstly the single walk velocities of the normal people and the imitated elderly people through measuring the single travel times from the start line to the goal line was measured. Over 216 single walk velocities for the normal people and 72 ones for the imitated elderly people were taken and averaged.

The average walk velocities for the normal people and the imitated elderly people were 1.338 m/s and 0.899 m/s, respectively. However, the lowest walk velocities were 0.95 m/s and 0.29 m/s, while the highest values were 2.07 m/s and 1.45 m/s, respectively. Thus, the distributions of walk velocities for both were rather wide; the standard deviations for the normal people and the imitated elderly people were 0.171 and 0.247, respectively.

When the unidirectional pedestrian flow experiment was performed, there were 24 pedestrians including 16 normal people and 8 imitated elderly people distributed in the start zone, shown in Fig. 1. At time $t = 0$, the pedestrians begin to move to the right from the left; as soon as they reach the goal line, they are removed from the channel. We used the video camera to observe all the pedestrians present within the channel. By a careful analysis of the video recordings, we determined the trajectory.

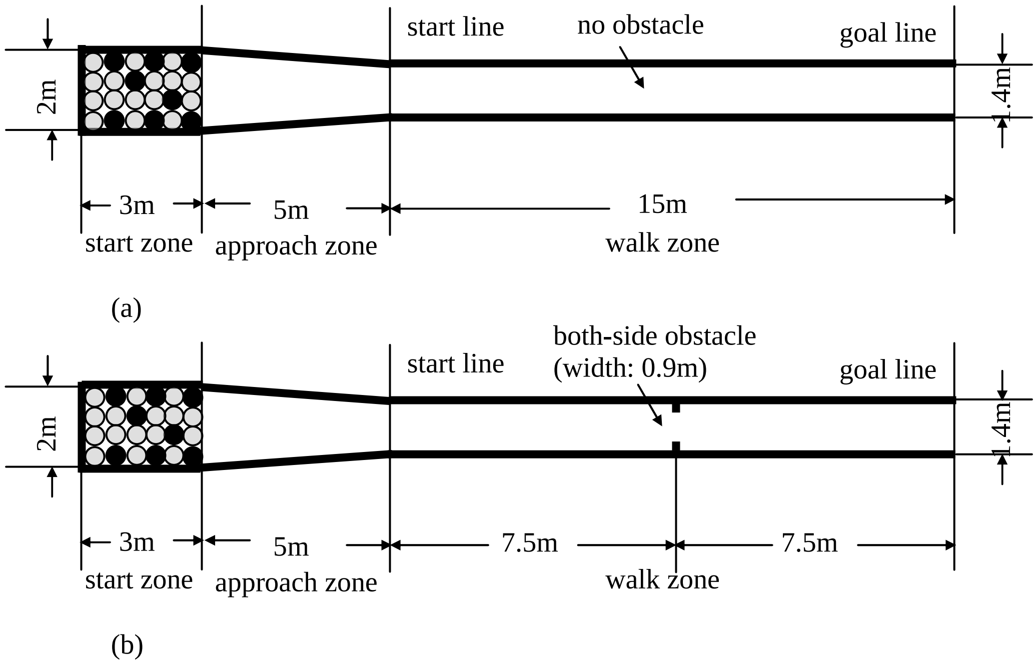

FIGURE 1. Schematic illustration of the unidirectional pedestrian flow. In the start zone with $L_s = 3$ m and $W_s = 2$ m, pedestrians with two different walk velocities are distributed with a certain pattern. The dark full circle represents the normal people, and the black one indicates the elderly people. In the walk zone of length $L_w = 15$ m and width $W_w = 1.4$ m, there are two situations including (a) no obstacle and (b) both-side obstacle with width of 0.9 m. The pedestrians move to the right from the left; when they reach the goal line, they are removed from the channel. It is noted that there is an approach zone of length $L_a = 5$ m to allow pedestrians to adjust to the 1.4 m width from that of 2 m width.

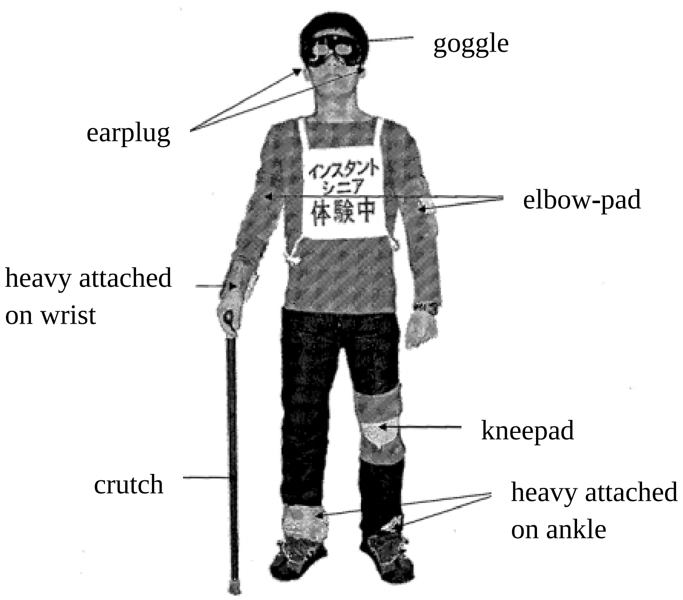

FIGURE 2. Normal people with special equipment to imitate elderly people. The equipment is used not only to make normal people walk slowly, but also to describe the elderly people's other characteristics, i.e. some blind and deaf, etc.

TABLE 1. Comparison of the mean individual travel time between experiment, averaged over 3 samples, and simulation with three kinds of numbers of small grids at an update time-step, averaged over 100 simulations. The numbers on the white background are for the normal people, and the ones on the gray background are for the imitated elderly people. It should be noted that the travel time was defined as the time that the pedestrian walked between the start line and the goal line.

Experiment							Simulation (1 small grid)					
no obstacle												
16.79	16.92	15.41	16.19	14.42	15.36		17.33	18.35	17.70	18.31	16.54	17.47
16.85	15.90	15.85	13.81	13.28	11.84		16.81	17.27	18.42	14.67	11.40	11.25
15.96	16.01	15.20	15.00	14.66	11.87		16.84	16.47	15.90	15.57	17.97	11.25
16.19	15.96	15.62	14.20	13.35	14.29		17.27	18.17	17.66	18.08	16.58	17.35
both-side obstacle												
21.03	21.23	17.65	17.86	16.13	16.43		19.34	22.28	20.43	21.92	18.73	18.36
21.23	21.85	19.07	16.37	14.75	12.26		18.05	18.93	21.46	15.03	11.40	11.60
21.33	19.91	18.37	17.12	16.01	12.50		18.21	17.86	18.21	15.86	18.46	11.47
21.53	20.74	18.44	17.24	14.24	15.10		20.32	22.35	19.54	22.17	17.57	18.11
Simulation (3 small grids)							Simulation (9 small grids)					
no obstacle												
17.76	17.95	18.01	18.13	16.63	17.39		18.11	18.66	17.70	18.33	17.12	18.27
17.10	18.11	18.99	15.70	12.20	12.15		17.82	18.17	18.42	14.67	12.31	13.11
17.14	16.76	16.12	15.77	17.37	11.78		17.67	17.41	15.91	15.57	18.12	12.75
17.65	18.28	16.96	18.14	17.35	17.85		19.12	18.57	17.16	18.08	16.75	18.15
both-side obstacle												
19.74	22.20	20.79	21.12	18.99	18.96		20.89	23.48	20.98	22.10	18.77	19.16
18.61	19.11	21.56	15.22	12.20	12.10		20.11	19.73	21.41	15.93	11.21	12.12
18.78	18.05	18.12	15.91	18.76	11.89		20.62	19.16	19.54	16.96	19.16	12.07
20.90	21.98	20.01	21.97	17.17	18.81		21.92	23.53	20.14	22.88	18.19	19.01

There were six students each with four stopwatches for each row went with the pedestrians for measuring travel times from the start line to the goal line. The individual travel time was defined as the time that the pedestrian walked between the start line and the goal line. Table 1 gives the comparison of the mean individual travel time between experiment, averaged over 3 samples, and simulation with three kinds of numbers of small grids at an update time-step, averaged over 100 simulations. The left top parts are experimental data. The numbers on the white background are for the normal people, and the ones on the gray background are for the imitated elderly people. It should be noted that the datum times in Table 1 and Fig. 2 are different, the first is at start line, and the second is at beginning of experiment. Table 2 is the mean travel time of 24 pedestrians including 16 normal people and 8 imitated elderly people from experimental data and simulation results. According to the single walk velocities, the single travel times were 11.21 s and 16.69 s, respectively. The mean travel time of 16 normal people and 8 imitated elderly people was 13.04 s if not considering the interaction among pedestrians. The values in Table 2 are all larger than 13.04 s, which means the interaction among pedestrians makes the pedestrians walk slowly. It is also indicated from Table 2 that the mean travel times for both-side obstacle in the walk zone is more than those for no obstacle. It accords well with the practical phenomenon that obstacles slow down pedestrians' walking.

TABLE 2. Mean travel time of 24 pedestrians including 16 normal people and 8 imitated elderly people from experimental data and simulation results

	Experiments	Simulation (1 small grid)	Simulation (3 small grids)	Simulation (9 small grids)
no obstacle	15.04	16.44	16.72	17.00
both-side obstacle	17.85	18.24	18.46	19.13

MODEL

In the following, the outline of the motor schema-based cellular automaton model [9] for pedestrian and evacuation dynamics will be given, which allows reproduction of our experimental findings for the unidirectional pedestrian flow with different walk velocities. In this model, the cell size was chosen as 0.45m, which accords to the pedestrian occupancy from the observation of experiments.

In the CA model, a rule defines the state of a site in dependence of the neighbour of the site. Generally the state of the core site at the next update time-step depends on the states of the sites in the neighbour including the site above, below, right and left, also the core site itself, of this update time-step. Each pedestrian is only allowed to move to a neighbour site in the directions of East, West, South and North at a given update time-step. In each update time-step, for each pedestrian a desired move is chosen according to the walk weights of four directions. The walk weights are determined based on motor schema described below.

From the experimental observation and with the motor schema-based CA model, pedestrian walk can be divided into three basic behaviors, i.e. “move-to-goal” (moves to the given direction), “avoid-away” (avoids other pedestrians or obstacles) and “avoid-around” (gets ahead of other pedestrians with low velocity or avoids around obstacles) basic behaviors. For simplicity, the magnitudes of three basic behaviors are set as 1, i.e. $\left|\vec{S}_{goal}\right| = \left|\vec{S}_{away}\right| = \left|\vec{S}_{around}\right| = 1$. The direction of “move-to-goal” basic behavior is along a line from pedestrian to the goal, moving to the goal. It is obvious that all pedestrians have the “move-to-goal” basic behavior. The direction of “avoid-away” is along a line from the pedestrian to the center of another pedestrian or obstacle, and moving away from the obstacle. The direction of “avoid-around” basic behavior is perpendicular to that of “avoid-away”. It has two directions; which is chosen depends on the kinds of moving pedestrian and encountered obstacles. In the situations, it has two conditions: (1) If any pedestrian encounters obstacles, the direction of the “avoid-around” basic behavior points to the center line with $W_w/2$; (2) If the normal people encounters the imitated elderly people, we choose a stochastic one for the direction of the “avoid-around” basic behavior. These basic behaviors are independent, they can run concurrently. The importance of basic behaviors relative to each other is indicated by a weight for each one, i.e. W_{goal}, W_{away} and W_{around} are for the “move-to-goal”, “avoid-away” and “avoid-around” basic behaviors, respectively. This paper set the weights similar and as 1 for simplifying the update rules considering experimental observations. Each vector of basic behavior is multiplied by the corresponding weight. And the walk weights of four directions are the sum of these products in the corresponding directions.

The update rules of the motor schema-based CA model have the following structure [9]:

(1) The walk weights of a pedestrian are computed based on behaviorism described above.
(2) If the direct neighbour in a direction is occupied by another pedestrian or obstacle, its walk weight in the corresponding direction is set to be zero.
(3) The pedestrian will walk in the direction whose walk weight is the biggest among four directions. If there are many walk weights are similar, the pedestrian will choose stochastic one.
(4) If the walk weights of four directions are all zero, the pedestrian will not walk.

In this model, sequential update is chosen since the pedestrians walked asynchronously in experiments[9]. In each update time-step, the pedestrians are numbered randomly from 1 to N, where N is the total number of pedestrians in the system, and then each pedestrian is updated once in the sequential order from 1 to N.

In this paper we carry out small grid analysis of the above presented model, shown in Fig.3. We divide the occupied space of a walker into 9*9 small grids in simple form considering numerical accuracy and computational efficiency because smaller grids result in more computation time. Fig. 3 shows the traditional model and its small grid analysis. In small grid analysis, the walker can move one or many small grids (1/9 grid in Fig. 3(b)) at an update time-step.

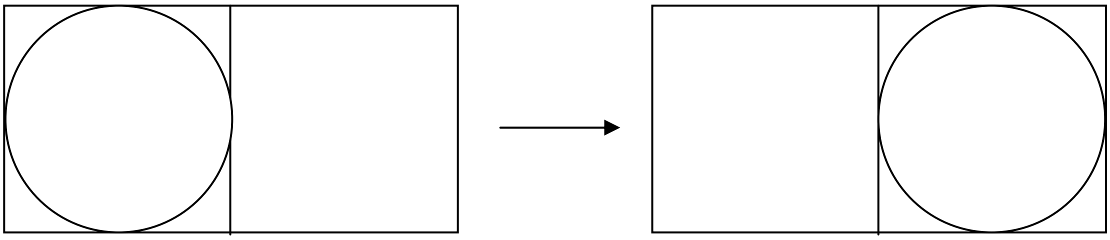

(a) The traditional model. The cell grid is 0.45*0.45m^2. The pedestrian moves a grid at an update time-step, that is 0.45 m/step.

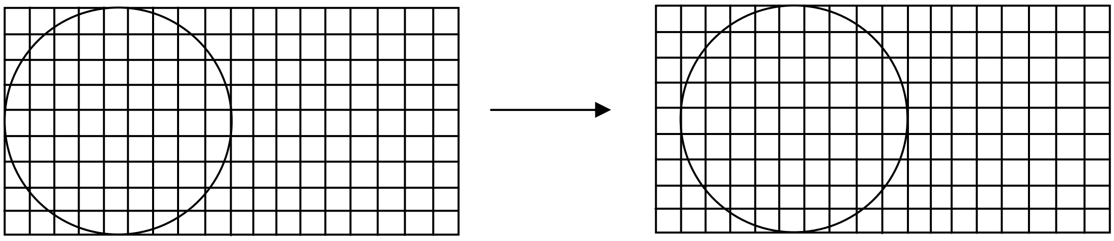

(b) Small grid analysis. The pedestrian moves a small grid (1/9 grid) at an update time-step, that is 0.05 m/step

FIGURE 3. The traditional model and its small grid analysis

For small grid analysis, the effects of different numbers of small grid at an update time-step with the same desired walk velocity were examined, on the travel time from start line to goal line of unidirectional pedestrian flow. For simulating the pedestrian flow with different walk velocities, we introduce an idea for the model, i.e. pedestrians update at different time-step intervals [13]. The normal people update at every 6 time-steps, and the imitated elderly people update at every 9 time-steps. For different numbers of small grid at an update time-step, we set that the pedestrian spends 1/160, 3/160 and 9/160 s at an update time-step corresponding to 1, 3 and 9 small grids at an update time-step, respectively. Thus in this model, the single walk velocities for the normal people and the imitated elderly people are 1.333 m/s and 0.889 m/s, which are similar to the experimental walk velocities of 1.338 m/s and 0.899 m/s, respectively.

Table 1 also gives the simulation results of the mean individual travel time with three kinds of numbers of small grids at an update time-step (1, 3 and 9), averaged over 100 simulations. The numbers on the white background are for the normal people, and the ones on the gray background are for the imitated elderly people. Table 2 is the comparison of the mean travel time of 24 pedestrians including 16 normal people and 8 imitated elderly people for different distribution patterns and obstacles. It is clear that the travel time is different with the different numbers of small grid at an update time-step though their desired walk velocity is similar; it is believed that the travel time is sensitive to the number of small grid at an update time-step, and the travel time is constant when the number of small grid at an update time-step reaches a critical value [12]. From Table 1 and Table 2, it is surprisingly indicated that the simulation results with one small grid at an update time-step agree well with the experimental data. Thus the simulations presented here reproduce the experimental observations not only qualitatively, but even in a quantitative way. It is illustrated that the presented motor schema-based cellular automaton model with an appropriate small grid at an update time-step is efficient in the simulation of pedestrian flow and is a useful tool for fire safety research and management.

CONCLUSIONS

This paper presents small grid analysis of motor schema-based cellular automaton model for pedestrian and evacuation dynamics. Experiments of unidirectional pedestrian flow with different walk velocities were carried out to validate the presented model. In the model, each pedestrian is treated as an intelligent mobile robot, and motor schemas including move-to-goal, avoid-away and avoid-around drive pedestrians to interact with their environment. Small grid analysis of this model for the check of the effect of different numbers of small grid at an update time-step with the same desired walk velocity, on the travel time, is conducted. In experiments, the lower walk velocity was provided by the normal people with special equipment, which made them walk slowly, to imitate the elderly people. Travel time of each pedestrian from start line to goal line with different initial distribution patterns and obstacles in the way was measured to compare with simulation results. Conclusions can be drawn below:

(1) The travel time is sensitive to the number of small grid at an update time-step in CA model.
(2) The simulation results with one small grid at an update time-step agree well with the experimental data.
(3) It is believed that the presented motor schema-based cellular automaton model with an appropriate small grid at an update time-step is efficient in the simulation of pedestrian flow and is a useful tool for fire safety research and management.

ACKNOWLEDGEMENTS

The authors would like to acknowledge the students in Prof. Hasemi's Laboratory for experiments, and the supports provided by the Program for New Century Excellent Talents in University (NCET), Ministry of Education.

REFERENCES

1. Nagatani, T., "Dynamical Transition and Scaling in a Mean-field Model of Pedestrian Flow at a Bottleneck", Physica A, 300, 558-566, 2001.
2. Maniccam, S., "Effects of Back Step and Update Rule on Congestion of Mobile Objects", Physica A, 346, 631-650, 2005.
3. Tajima, Y. and Nagatani, T., "Scaling Behavior of Crowd Flow outside a Hall", Physica A, 292, 545-554, 2001.
4. Lo, S.M., Fang, Z., Lin, P. and Zhi, G.S., "An Evacuation Model: the SGEM Package", Fire Safety Journal, 39, 169-290, 2004.
5. Zhang, P.H., Huang, X.Y., Lo, S.M. and Zhong, M.H., "Agent-based Dynamic Model for Pedestrian Counter Flow", Fire Safety Science - Proceedings of the Eighth International Symposium, Beijing, 581-590, 2005.
6. Burstedde, C., Klauck, K., Schadschneider A. and Zittartz, J., "Simulation of Pedestrian Dynamics using a 2-dimensional Cellular Automaton", Physica A, 295, 507-525, 2001.
7. Kirchner, A. and Schadschneider, A., "Simulation of Evacuation Processes using a Bionics-inspired Cellular Automaton Model for Pedestrian Dynamics", Physica A, 312, 260-276, 2002.
8. Kirchner, A., Kluepfel, H., Nishinari, K., Schadschneider, A. and Schreckenberg, M., "Discretization Effects and Influence of Walking Speed in Cellular Automata Models for Pedestrian Dynamics", Journal of Statistical Mechanics: Theory and Experiment, P100011, 2004.
9. Weng, W.G., Hasemi, Y. and Fan, W.C., "Motor Schema-based Cellular Automaton Model for Pedestrian Dynamics", International Journal Modern Physics C, 17, 853-859, 2006.
10. Brooks, R., "A Layered Intelligent Control System for a Mobile", IEEE Transaction on Robotics and Automation, 2, 14-23, 1986.

11. Arkin, R.C., “Motor Schema-based mobile Robot Navigation”, International Journal of Robotics Research, 8, 92-112, 1989.
12. Weng, W.G., Pan, L.L., Shen, S.F. and Yuan, H.Y., “Small Grid Analysis of Discrete Model for Evacuation from a Hall”, Physica A, 374, 821-826, 2007.
13. Weng, W.G., Chen, T., Yuan, H.Y. and Fan, W.C., “Cellular Automaton Simulation of Pedestrian Counter Flow with Different Walk Velocities”, Physical Review E, 74, 036102, 2006.